# Quantum Chemistry Investigation of Fluorinated Polymer Systems of Industrial Interest

Evangelos Mavroudakis,[†] Danilo Cuccato,[†] Marco Dossi,[‡] Giovanni Comino,[‡] and Davide Moscatelli*[,†]

[†]Dipartimento di Chimica, Materiali e Ingegneria Chimica "Giulio Natta", Politecnico di Milano, 20131 Milano, Italy

[‡]Solvay Specialty Polymers Italy S.p.A., Viale Lombardia 20, 20021 Bollate, Italy

## INTRODUCTION

Fluorinated polymers are extremely interesting polymeric materials containing fluorine atoms in their chemical configurations. There are two different types of fluorinated polymers: the perfluoropolymers and the partially fluorinated polymers. In the perfluoropolymers, there are no hydrogen atoms in the structure, whereas in the partially fluorinated polymers, only some of the hydrogen atoms in the analogous hydrocarbon configurations are replaced by fluorine atoms.

Fluoropolymers exhibit versatile combinations of properties; they vary from elastomers and thermoplastics to completely amorphous polymers, exhibiting remarkable resistance against thermal, chemical, mechanical, and aging stresses.[1−4] The outstanding properties that fluoropolymers possess are most likely linked to the low polarizability and the strong electronegativity of the fluorine atom due to its small van der Waals radius (1.32 Å) and the strong C−F bond (485 kJ·mol$^{-1}$).[5] Fluoropolymers that contain VDF exhibit excellent weather durability, low flammability, low surface energy, and acid resistance in addition to the above-mentioned resistances.[6,7] Therefore, these polymers are suitable for applications in many different fields, such as aerospace, aeronautics, and energy, as well as in the chemical, electronic, and construction industries.[8−11]

Achieving the desired combination of properties in homopolymers is often difficult. However, using the proper monomer mixtures may generate fluorinated copolymers that assume all of the required properties while overcoming the drawbacks of homopolymers. A large number of scientific studies have been focused on the investigation of properties and on the determination of structures of VDF, HFP, and TFE binary copolymers or terpolymers. Ameduri collected most of these studies in his review.[5] Especially for the fluorinated copolymers containing VDF, many studies based on high resolution $^{19}$F and $^{1}$H nuclear magnetic resonance (NMR) spectroscopy have been conducted to elucidate the structure and the comonomer sequences in the polymer chain. The VDF monomer units may be found in two different orientations in the polymer chain, meaning that during the propagation, VDF may occur in the normal head-to-tail (−$CH_2CF_2$−$CH_2CF_2$−), as well as the reversed head-to-head (−$CH_2CF_2$−$CF_2CH_2$−) and tail-to-tail (−$CF_2CH_2$−$CH_2CF_2$−), directions. The defects in the structures (head-to-head and tail-to-tail) depend on the processing conditions and temperatures, whereas the percentage of reversed VDF units may affect the final polymer properties.[12−18] Despite the wide application range for these polymers and the industrial interest in knowledge of their polymerization kinetics, the data in the literature are still inadequate. Some research groups measured the reactivity ratios in the copolymerizations of VDF with HFP and TFE,[19−21] and a mathematical model was developed by Apostolo et al. for the kinetics description of the emulsion polymerization of VDF and HFP.[22] Recently, the

**Received:** September 19, 2013
**Revised:** December 11, 2013
**Published:** December 11, 2013

copolymerization propagation rate coefficients $k_{p,cop}$ for the homogeneous phase copolymerization of VDF with HFP in supercritical $CO_2$ was proposed by Siegmann et al.[23]

This work focuses on the computational investigation of the kinetic coefficients for all of the propagation reactions involved in VDF homopolymerization and in the binary copolymerization systems of VDF/HFP, VDF/TFE, and HFP/TFE. All the optimal monomer, radical, and polymer structures were detected using quantum mechanics calculations based on DFT and later these structures were used to calculate the kinetic constants. The copolymer systems involving VDF have been studied during both the normal and the reverse monomer addition. Arrhenius kinetic parameters for all of the addition reactions involved in each copolymer system were estimated computationally and the kinetic coefficients have been calculated at 60 °C. Copolymer compositions and propagation rate coefficients versus monomer mole fraction graphs for all the copolymer systems were created by computationally estimating the kinetic constants at 60 °C. The activation energy along with temperature dependent pre-exponential factor values were proposed for all of the propagation reactions of the studied copolymer systems. The knowledge of the Arrhenius parameters for the reactions of the above-mentioned systems may be a great asset during the production of specialty fluoropolymer materials with the desired composition and therefore with the desired properties.

## THEORY AND COMPUTATIONAL METHODS

**A. Terminal Model.** All the kinetic constants obtained using the quantum mechanics (QM) simulations have been calculated according to the TM. This model assumes that the reactivity ratio of each propagation reaction depends only upon the terminal unit of the growing chain and therefore a simple scheme composed of four reactions (Scheme 1) is sufficient to describe a copolymer system.

**Scheme 1. Elementary Reactions Involved in Determining the Monomer Reactivity Ratios of Copolymer Systems According to the TM**

$$\cdots A^{\cdot} + A \xrightarrow{k_{AA}} \cdots AA^{\cdot}$$

$$\cdots A^{\cdot} + B \xrightarrow{k_{AB}} \cdots AB^{\cdot}$$

$$\cdots B^{\cdot} + A \xrightarrow{k_{BA}} \cdots BA^{\cdot}$$

$$\cdots B^{\cdot} + B \xrightarrow{k_{BB}} \cdots BB^{\cdot}$$

After the estimation of the kinetic coefficients, monomer reactivity ratios $r_A$ and $r_B$ can be calculated as defined in eqs 1 and 2.

$$r_A = \frac{k_{AA}}{k_{AB}} \tag{1}$$

$$r_B = \frac{k_{BB}}{k_{BA}} \tag{2}$$

Usually a binary copolymer system according to the TM can be fully described by the above-mentioned scheme. However, that is not the case for the binary copolymer systems involving VDF. As was previously mentioned, two different VDF radicals lead to defect structures. The presence of these two different radicals turns each copolymer system, including VDF, into a pseudoterpolymer system. All VDF copolymer systems were studied like the terpolymer systems. For terpolymerization, the kinetic scheme that describes the systems is more complicated. Alfrey et al.[24] demonstrated that there are nine important propagation reactions used to determine the terpolymer composition (Scheme 2). Using the kinetic coefficients for the

**Scheme 2. Elementary Reactions Involved in Determining the Monomer Reactivity Ratios of Terpolymer Systems According to the TM**

$$\cdots A^{\cdot} + A \xrightarrow{k_{AA}} \cdots AA^{\cdot}$$

$$\cdots A^{\cdot} + B \xrightarrow{k_{AB}} \cdots AB^{\cdot}$$

$$\cdots A^{\cdot} + C \xrightarrow{k_{AC}} \cdots AC^{\cdot}$$

$$\cdots B^{\cdot} + A \xrightarrow{k_{BA}} \cdots BA^{\cdot}$$

$$\cdots B^{\cdot} + B \xrightarrow{k_{BB}} \cdots BB^{\cdot}$$

$$\cdots B^{\cdot} + C \xrightarrow{k_{BC}} \cdots BC^{\cdot}$$

$$\cdots C^{\cdot} + A \xrightarrow{k_{CA}} \cdots CA^{\cdot}$$

$$\cdots C^{\cdot} + B \xrightarrow{k_{CB}} \cdots CB^{\cdot}$$

$$\cdots C^{\cdot} + C \xrightarrow{k_{CC}} \cdots CC^{\cdot}$$

reactions presented in Scheme 2, six monomer reactivity ratios may be calculated (eqs 3–8).

$$r_{AB} = \frac{k_{AA}}{k_{AB}} \tag{3}$$

$$r_{BA} = \frac{k_{BB}}{k_{BA}} \tag{4}$$

$$r_{AC} = \frac{k_{AA}}{k_{AC}} \tag{5}$$

$$r_{CA} = \frac{k_{CC}}{k_{CA}} \tag{6}$$

$$r_{BC} = \frac{k_{BB}}{k_{BC}} \tag{7}$$

$$r_{CB} = \frac{k_{CC}}{k_{CB}} \tag{8}$$

The kinetic coefficients and the monomer reactivity ratios used by the proper mathematical models based on population

balance equations may provide compositional information for the obtained polymer in both co- and terpolymer systems; they may also be used to estimate the average propagation rate coefficients ($k_{p,cop}$ and $k_{p,ter}$). Given that the propagation reactions dominate, the monomer consumption for a copolymerization may be defined as follows:

$$\frac{dM}{dt} = (k_{pAA}p_A + k_{pBA}p_B)AR^\bullet + (k_{pBB}p_B + k_{pAB}p_A)BR^\bullet = k_{p,cop}MR^\bullet \quad (9)$$

Copolymerization average propagation rate coefficient and copolymer composition can be described as follows:

$$k_{p,cop} = \frac{(k_A^*A + k_B^*B)}{M} \quad (10)$$

$$F_A = \frac{k_A^*A}{k_A^*A + k_B^*B} \quad (11)$$

where

$$k_A^* = k_{pAA}p_A + k_{pBA}p_B \quad (12)$$

$$k_B^* = k_{pBB}p_B + k_{pAB}p_A \quad (13)$$

$$p_A = A^\bullet/R^\bullet \quad (14)$$

$$p_B = B^\bullet/R^\bullet \quad (15)$$

where $A$ is the concentration of monomer A, $B$ is the concentration of monomer B, $M$ is the total monomer concentration, $A^\bullet$ is the concentration of radical A, and $B^\bullet$ is the concentration of radical B.

Accordingly, for a terpolymerization, the overall terpolymer kinetic coefficient may be calculated as follows:

$$k_{p,ter} = \frac{(k_A^*A + k_B^*B + k_C^*C)}{M} \quad (16)$$

And the terpolymer composition may be described as follows:

$$F_A = \frac{k_A^*A}{k_A^*A + k_B^*B + k_C^*C} \quad (17)$$

In this case, the pseudopropagation rate constants $k_A^*$, $k_B^*$, and $k_C^*$ are defined as follows:

$$k_A^* = k_{pAA}p_A + k_{pBA}p_B + k_{pCA}p_C \quad (18)$$

$$k_B^* = k_{pAB}p_A + k_{pBB}P_B + k_{pCB}p_C \quad (19)$$

$$k_C^* = k_{pAC}p_A + k_{pBC}p_B + k_{pCC}p_C \quad (20)$$

$$p_C = C^\bullet/R^\bullet \quad (21)$$

where $A$ is the concentration of monomer A, $B$ is the concentration of monomer B, $C$ is the concentration of monomer C, $M$ is the total monomer concentration, $A^\bullet$ is the concentration of radical A, $B^\bullet$ is the concentration of radical B, and $C^\bullet$ is the concentration of radical C.

**B. Quantum Mechanics.** The exchange and correlation energies were calculated using a computational approach based on DFT. All of the reactant and product conformations were optimized using the Becke three-parameter and Lee–Yang–Parr functional (B3LYP). Quantum chemical calculations for radicals were performed using a spin multiplicity of 2 and an unrestricted wave function (UB3LYP). Many functionals may be used to describe radical addition reactions; however, the B3LYP method was adopted because it provides excellent low-cost performance, as demonstrated in previous literature reports.[25−36] Even though B3LYP is less accurate when predicting electronic energies compared to other hybrid density functionals,[37,38] nonsystematic errors are absent in DFT methods and this was demonstrated when the radical addition to double bonds was studied;[34,39] these results led us to choose this method to determine the kinetic coefficients of fluorinated polymer systems propagation reactions. Simulations were performed using the all-electron 6-31 basis set with added polarization functions (6-31G(d,p)). To obtain an accurate description of the investigated compounds' molecular structures, a broad structural optimization was performed to detect the absolute energy minimum conformations; in particular, the potential energy surface (PES) of each possible dihedral angle rotation was determined for each reactant, product and transition state; the obtained absolute minimum geometries were adopted for the final optimizations. This procedure was proven adequate to discern the optimal structures.[35] The geometry of each molecular structure (reactants, transition states, and products) was considered stable only after calculating the vibrational frequencies and force constants and if no imaginary vibrational frequency was found. Transition state structures were located by adopting the synchronous transit-guided quasi Newton method and are characterized by a single imaginary vibrational frequency. Later a combined B3LYP/MPWB1K approach was used during the second estimation of the kinetic constants. In particular, after the geometric optimizations, frequency calculations, and identification of the transition state locations were conducted at the B3LYP level,[40,41] the hybrid meta DFT method, MPWB1K was used to perform single point calculations to evaluate the electronic and zero-point energies.[42] The corresponding kinetic constants in both cases were determined using the classical transition state theory (TST) as follows:

$$k(T) = A\cdot e^{-E_a/k_bT} = \frac{k_bT}{h}\cdot\frac{Q^{\neq}}{Q^R}\cdot e^{-E_a/k_bT} \quad (22)$$

where $k_b$ and $h$ are the Boltzmann and Planck constants, respectively; in addition, $T$ is the temperature, $E_a$ is the activation energy of the process calculated from the difference between the electronic energy of the TS and the energy of the reactants (including zero-point energy), and $Q$ represents the product of the partition functions ($q^{trans}$, $q^{vib}$, $q^{rot}$, $q^{el}$) for the transition states ($\neq$) and reactants (R). In particular, $q^{el}$ is the electronic partition function whereas $q^{trans}$, $q^{vib}$, and $q^{rot}$ are the translational, vibrational, and rotational partition functions, respectively, calculated according to the following equations:

$$q^{trans} = \frac{(2\pi m k_bT)^{3/2}}{h^3}V \quad (23)$$

$$q^{vib} = \prod_{i=1}^{N_{vib}} \frac{1}{1 - \exp\left(-\frac{h\nu_i}{k_bT}\right)} \quad (24)$$

$$q^{rot.} = \frac{8\pi^2(2\pi k_bT)^{3/2}\sqrt{I_xI_yI_z}}{\sigma h^3} \quad (25)$$

where $V$ is the volume, $m$ is the particle mass, $v_i$ is the vibrational frequency, $I_xI_yI_z$ are the rotational constants, and $\sigma$ is the rotational symmetry number. The harmonic oscillator (HO) model has been used for the ab initio calculations of the partition functions. In the literature can be found studies where the hinder rotor (HR) model was used to model vibrational modes for propagation reactions;[28,34,38,43] however, the evaluation of the internal rotation partition function according to the HR is not necessary for this study because most of the rotations are on the backbone. Furthermore the correction of the rate coefficients that HR can provide for relative low temperatures is not of great importance.[44,45] All of the quantum chemistry calculations were performed using the Gaussian 09 program suite and all pictures were drawn using Molden 4.2.[46,47]

**Scheme 3. (a) VDF Monomer, (FH, HF), (b) VDF Radical on Head ($HF^{\bullet}$), and (c) VDF Radical on Tail ($FH^{\bullet}$)**

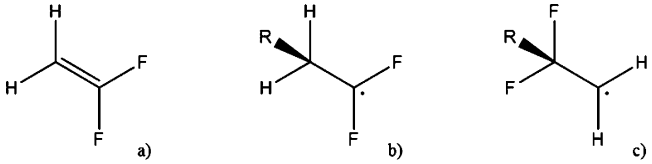


**Scheme 4. Elementary Reactions Involved in the Pseudo Copolymerization of VDF According to the TM**

$$\cdots FH^{\cdot} + FH \xrightarrow{k_{FH-FH}} \cdots FH - FH^{\cdot}$$

$$\cdots FH^{\cdot} + HF \xrightarrow{k_{FH-HF}} \cdots FH - HF^{\cdot}$$

$$\cdots HF^{\cdot} + FH \xrightarrow{k_{HF-FH}} \cdots HF - FH^{\cdot}$$

$$\cdots HF^{\cdot} + HF \xrightarrow{k_{HF-HF}} \cdots HF - HF^{\cdot}$$

## RESULTS AND DISCUSSION

In the present study, the kinetic coefficients for all of the propagation reactions involved in each binary copolymerization system including VDF, HFP, and TFE, as well as the VDF homopolymerization, were estimated using quantum mechanics.

As observed in Scheme 3, there are two different VDF radicals;[5,17,48] therefore, the homopolymerization of VDF may be described by the four propagation reactions illustrated in Scheme 4.

The existence of these two different radicals indicates that four distinct reactions occur during the polymerization and changes the homopolymerization of VDF into a pseudo copolymer system. For the same reason, copolymer systems including VDF/HFP and VDF/TFE may be assumed to be pseudo terpolymer systems that may be described by the reactions presented in Scheme 2. For the last copolymer system, where the VDF monomer was not involved (i.e., HFP/TFE), the simple set of reactions reported in Scheme 1 describes the system. Detailed kinetic schemes for the above-mentioned systems can be found in the Supporting Information.

As was previously mentioned, all of the geometries used during the final optimization for every molecule were detected using a broad structural optimization. Using the HFP radical, the radical of HFP dimer, the radical of TFE dimer, and all the four possible dimer radicals of VDF as examples, the procedure used to investigate the best structures is presented. In Figure 1, the first structures used during the structural optimization of the above-mentioned molecules are presented. The potential energy surface for the dihedral angles assigned as rot. X (X:a-m) in Figure 1 are reported in Figure 2a–m.

The absolute minimum geometries (Figure 3) were then adopted for determining the kinetic constants. The same procedure was used to detect the required absolute minimum geometries for all of the radicals, monomers, and products involved in the propagation reactions illustrated in Schemes 4 and S1–S3 (Supporting Information).

The kinetic coefficients for the propagation reactions of the studied systems were estimated at 60 °C using two different

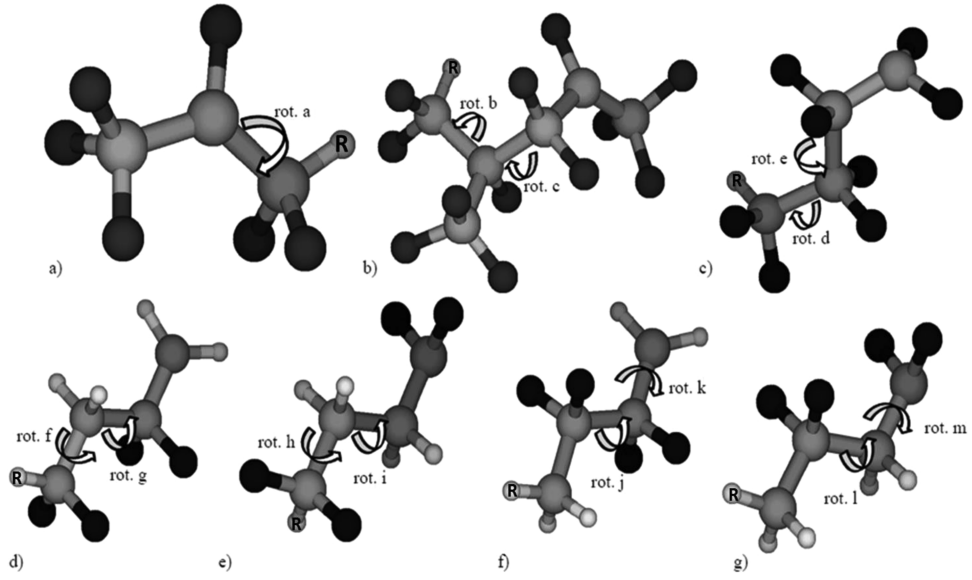


**Figure 1.** Molecular structures used to investigate the dihedral angle potential energy surfaces relative to the HFP and its dimer radical, as well as the TFE dimer and VDF dimer radicals.

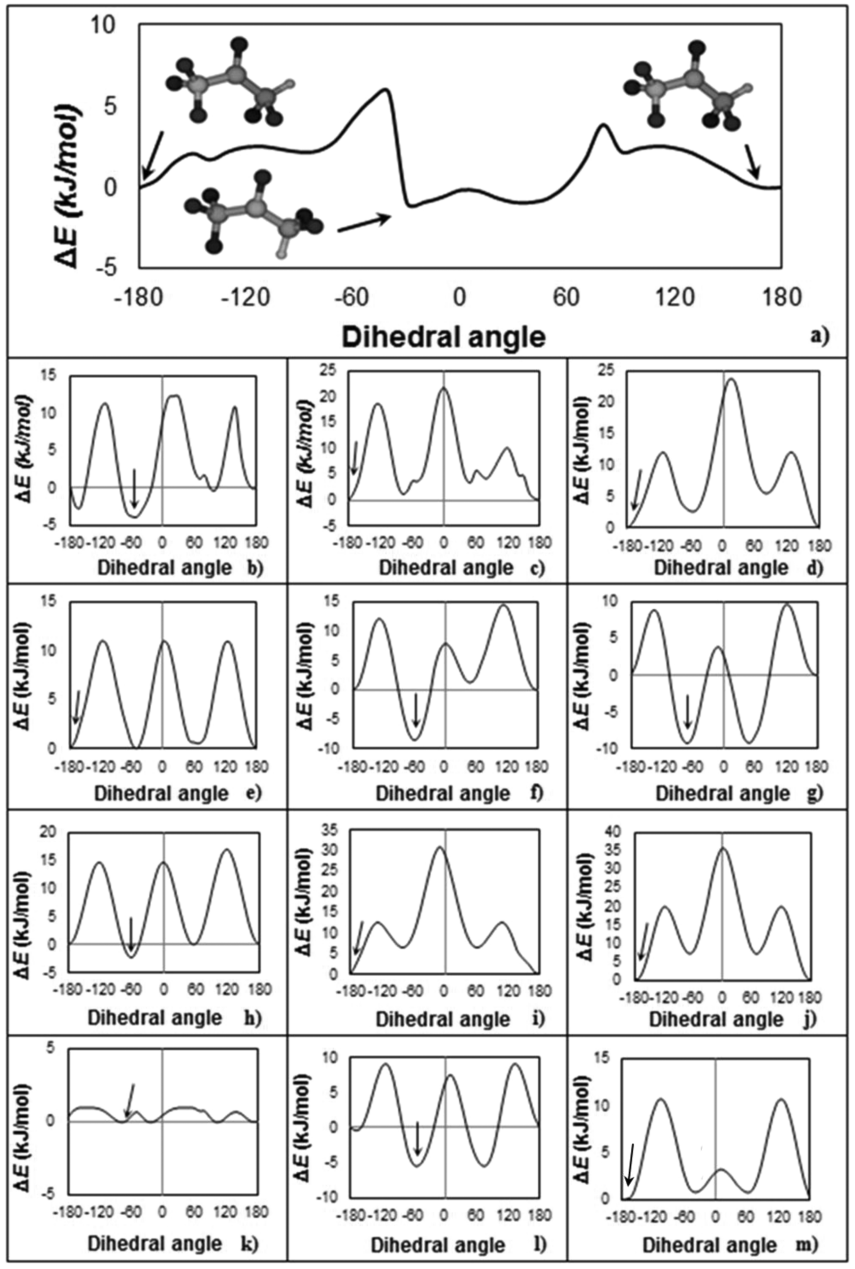


**Figure 2.** PES of dihedral rotation involved in the geometry optimization of the HFP, HFP dimer, TFE dimer, and VDF dimer radicals. The structures reported at 180° are relative to the geometries displayed in Figure 1, and the arrows point to the absolute minimum structures: (a) rot. a dihedral angle (Figure 1a); (b) rot. b dihedral angle (Figure 1b); (c) rot. c dihedral angle (Figure 1b); (d) rot. d dihedral angle (Figure 1c); (e) rot. e dihedral angle (Figure 1c); (f) rot. f dihedral angle (Figure 1d); (g) rot. g dihedral angle (Figure 1d); (h) rot. h dihedral angle (Figure 1e); (i) rot. i dihedral angle (Figure 1e); (j) rot. j dihedral angle (Figure 1f); (k) rot. k dihedral angle (Figure 1f); (l) rot. l dihedral angle (Figure 1g); (m) rot. m dihedral angle (Figure 1g).

levels of theory using and above-mentioned methodology. The terminal model has been applied for the simulations after the effect of the chain length had been studied and found within the uncertainty limits of the method. More details about this aspect can be found in the Supporting Information (Table S10). The results for the pseudo terpolymer system VDF/HFP calculated at the MPWB1K level of theory (The results at B3LYP level of theory are in the Supporting Information) are presented. In particular, Table 1 contains the reported Arrhenius parameters, whereas Table 2 reports the monomer reactivity ratios.

Using the estimated values presented in Tables 1 and 2, as well as in eqs 16 and 17, the terpolymer composition (Figure 4) and propagation rate coefficient (Figure 5) were reported versus the HFP molar monomer fraction.

The obtained value for the monomer reactivity ratio $r_{HF\_FH}$ indicates that for the homopolymerization of VDF more than 20% of the defects are expected for the backbone; however, to the best of our knowledge there are no experimental data from NMR studies for the VDF homopolymer. On the contrary, there are a few studies reporting the fraction of the head to head defects in the copolymer backbone.[5,22] The percentage of defect structures comprises between 2.8 and 7% depending on the copolymer system as well as the reaction conditions. Given that the VDF molar fraction in the copolymer mixtures is lower

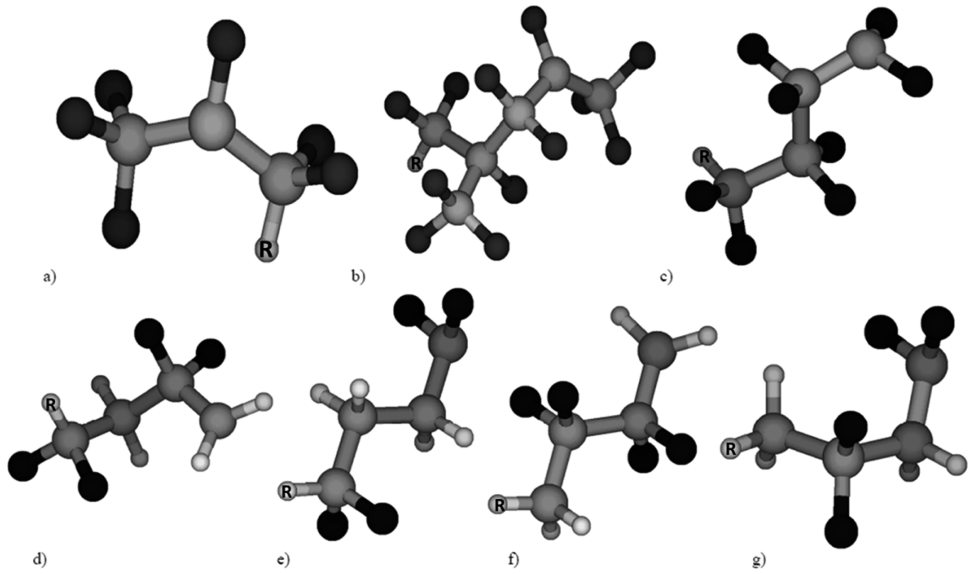


**Figure 3.** Molecular structures detected after structural optimization: (a) HFP, (b) HFP dimer, (c) TFE dimer, (d) VDF tail-to-head, (e) VDF tail-to-tail, (f) VDF head-to-head, and (g) VDF head-to-tail radicals.

**Table 1. Arrhenius Kinetic Parameters for the VDF/HFP Pseudo Terpolymerization at 60 °C**[a]

| | $E_a$ [kJ/mol] | $\log_{10}(A)$ | $k_{ij}$ [L/(mol·s)] |
|---|---|---|---|
| $HF^{\bullet}$ + HF → HF_$HF^{\bullet}$ | 20.52 | 6.621 | $2.53 \times 10^3$ |
| $HF^{\bullet}$ + FH → HF_$FH^{\bullet}$ | 18.20 | 6.042 | $1.54 \times 10^3$ |
| $HF^{\bullet}$ + HFP → HF_$HFP^{\bullet}$ | 7.22 | 5.755 | $4.19 \times 10^4$ |
| $FH^{\bullet}$ + HF → FH_$HF^{\bullet}$ | 13.03 | 6.293 | $1.78 \times 10^4$ |
| $FH^{\bullet}$ + FH → FH_$FH^{\bullet}$ | 26.58 | 5.680 | $3.26 \times 10^1$ |
| $FH^{\bullet}$ + HFP → FH_$HFP^{\bullet}$ | 19.87 | 5.541 | $2.66 \times 10^2$ |
| $HFP^{\bullet}$ + HF → HFP_$HF^{\bullet}$ | 0.54 | 5.245 | $1.45 \times 10^5$ |
| $HFP^{\bullet}$ + FH → HFP_$FH^{\bullet}$ | 15.92 | 4.123 | $4.24 \times 10^1$ |
| $HFP^{\bullet}$ + HFP → HFP_$HFP^{\bullet}$ | 12.60 | 3.848 | $7.45 \times 10^1$ |

[a]The rate coefficients were calculated at 60 °C. $FH^{\bullet}$: VDF tail radical. $HF^{\bullet}$: VDF head radical. HF, FH: VDF monomer. $HFP^{\bullet}$: HFP radical. HFP: HFP monomer. $k_{ij}$, i, j = FH, HF, HFP. The data represent the Arrhenius parameters determined using MPWB1K/6-31(d,p).

**Table 2. Monomer Reactivity Ratios for the VDF/HFP Pseudo Terpolymer System**[a]

| | |
|---|---|
| $r_{HF\_FH} = k_{HF\_HF}/k_{HF\_FH}$ | $1.64 \times 10^0$ |
| $r_{FH\_HF} = k_{FH\_FH}/k_{FH\_HF}$ | $1.83 \times 10^{-3}$ |
| $r_{HF\_HFP} = k_{HF\_HF}/k_{HF\_HFP}$ | $6.04 \times 10^{-2}$ |
| $r_{HFP\_HF} = k_{HFP\_HFP}/k_{HFP\_HF}$ | $5.14 \times 10^{-4}$ |
| $r_{FH\_HFP} = k_{FH\_FH}/k_{FH\_HFP}$ | $1.23 \times 10^{-1}$ |
| $r_{HFP\_FH} = k_{HFP\_HFP}/k_{HFP\_FH}$ | $1.76 \times 10^0$ |

[a]The data represent the monomer reactivity ratios determined using MPWB1K/6-31(d,p).

than the one of the homopolymer and that the defects are influenced by both polymerization process conditions and temperature, the proposed reactivity ratio for head to head addition seems to be reasonable.

The computational estimations at the B3LYP level of theory for the VDF/HFP system, as well as the computational results, the copolymer composition, and the overall copolymer or pseudo terpolymer propagation kinetic coefficient graphs for the rest of the studied systems at both levels of theory, are provided in the Supporting Information.

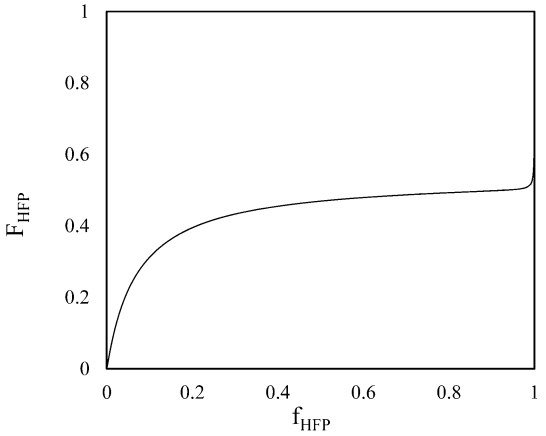


**Figure 4.** VDF/HFP pseudo terpolymer composition versus the HFP molar monomer fraction at 60 °C.

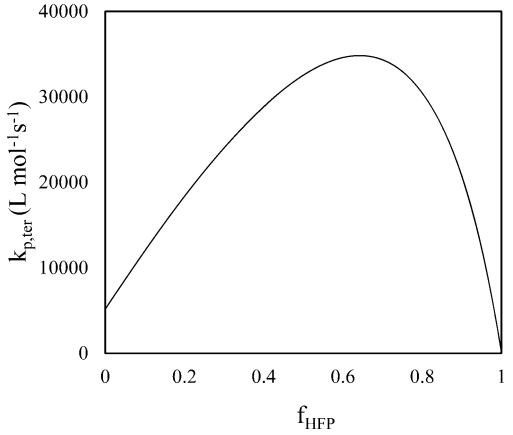


**Figure 5.** VDF/HFP pseudo terpolymer propagation rate coefficient versus the HFP molar fraction in the monomer phase at 60 °C.

To avoid associating the computational results with a specific temperature, the pre-exponential factor for the reactions was calculated at various temperatures; subsequently, the variables

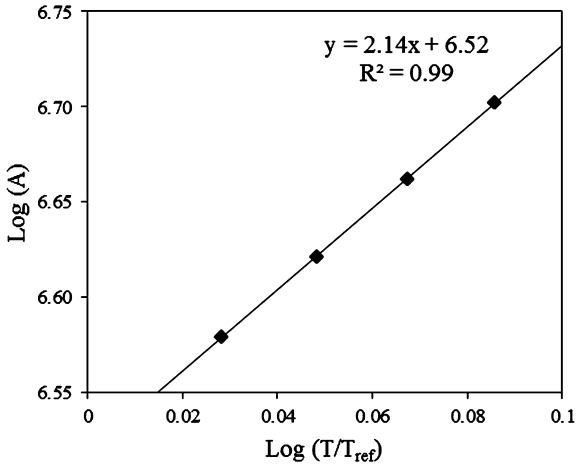


**Figure 6.** Interpolation of the computational values for the pre-exponential factor of the addition of the VDF radical on head to VDF monomer.

$A^*$ and $\alpha$ presented in eq 26 were estimated by interpolation using 298 K as the reference temperature. An example of the computations interpolation is provided in Figure 6.

$$A = A^* \cdot T^{*\alpha} \tag{26}$$

$$\log(A) = \log(A^*) + \alpha \cdot \log(T^*) \tag{27}$$

$$T^* = \frac{T}{T_{\text{ref}}} \tag{28}$$

The activation energies, $A^*$, and $\alpha$ factors for the propagation reactions involved with any possible copolymer, pseudo terpolymer, or terpolymer system are presented in Table 3. Using these values, the appropriate kinetic schemes, and proper mathematical models based on population balance equations, the polymer composition and the overall propagation kinetics coefficient for each co- or terpolymer system may be estimated at any temperature. Table 3 also reports the kinetic coefficients for the propagation reactions calculated at 60 °C.

The adopted computational method was validated for the pseudo terpolymer system, VDF/HFP. In particular, the kinetic coefficients for the terpolymer system were estimated within the 45−90 °C temperature range and the $k_{p,ter}$ were calculated when $f_{HFP}$ = 0.45. For the same temperature range and $f_{HFP}$ value, there are also experimental values for the $k_{p,ter}$ and Arrhenius parameters reported in literature.[23] In Figure 7, the computational estimations of $k_{p,ter}$ are reported along with the experimental data.

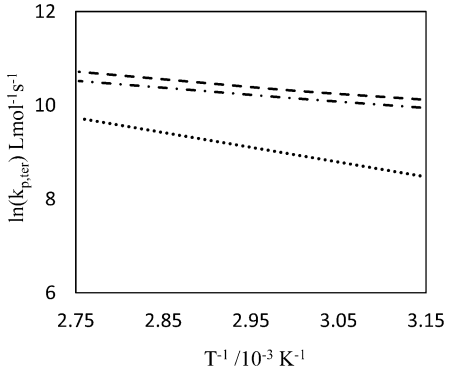


**Figure 7.** Temperature dependence of $k_{p,ter}$ for the VDF/HFP system. Linear fit for the experimental data (···, Siegmann et al.[23]); computational predictions at the B3LYP level of theory (−·−); computational predictions at the MPWB1K level of theory (− − −).

As observed in Figure 7, the computational predictions according to the TM at both the B3LYP and MPWB1K levels of theory are overestimating the experimental values. The computed value of the pseudo terpolymer propagation rate coefficient for $f_{HFP}$ = 0.45 at 60 °C as shown in Figure 5 is 30 000 L/(mol·s), whereas the experimental value for the same conditions is 7600 L/(mol·s). Given the uncertainties in both experiments and simulations and the different reaction environments ($CO_2$ for the experiments and vacuum for the simulations), a discrepancy of a factor of 4 could be considered

**Table 3. Arrhenius Kinetic Parameters for the Propagation Reactions Involved in Any Copolymer, Pseudo Terpolymer, or Terpolymer System Using VDF, HFP, or TFE Monomers**[a]

| | | $E_a$ [kJ/mol] | log($A^*$) | $\alpha$ | $k_{ij}$ [L/(mol·s)] |
|---|---|---|---|---|---|
| 1 | $HF^\bullet$ + HF → HF_$HF^\bullet$ | *20.52* | 6.52 | 2.14 | $2.53 \times 10^3$ |
| 2 | $HF^\bullet$ + FH → HF_$FH^\bullet$ | *18.20* | 5.94 | 2.09 | $1.54 \times 10^3$ |
| 3 | $HF^\bullet$ + HFP → HF_$HFP^\bullet$ | *7.22* | 5.64 | 2.33 | $4.19 \times 10^4$ |
| 4 | $FH^\bullet$ + HF → FH_$HF^\bullet$ | *13.03* | 6.22 | 1.48 | $1.78 \times 10^4$ |
| 5 | $FH^\bullet$ + FH → FH_$FH^\bullet$ | *26.58* | 5.61 | 1.43 | $3.26 \times 10^1$ |
| 6 | $FH^\bullet$ + HFP → FH_$HFP^\bullet$ | *19.87* | 5.46 | 1.67 | $2.66 \times 10^2$ |
| 7 | $HFP^\bullet$ + HF → HFP_$HF^\bullet$ | *0.53* | 5.15 | 1.88 | $1.45 \times 10^5$ |
| 8 | $HFP^\bullet$ + FH → HFP_$FH^\bullet$ | *15.92* | 4.04 | 1.72 | $4.24 \times 10^1$ |
| 9 | $HFP^\bullet$ + HFP → HFP_$HFP^\bullet$ | *12.60* | 3.75 | 1.97 | $7.45 \times 10^1$ |
| 10 | $HF^\bullet$ + TFE → HF_$TFE^\bullet$ | *9.97* | 6.25 | 2.43 | $6.40 \times 10^4$ |
| 11 | $FH^\bullet$ + TFE → FH_$TFE^\bullet$ | *16.36* | 6.07 | 1.86 | $3.96 \times 10^3$ |
| 12 | $TFE^\bullet$ + HF → TFE_$HF^{\bullet\bullet}$ | *14.25* | 6.46 | 2.23 | $2.18 \times 10^4$ |
| 13 | $TFE^\bullet$ + FH → TFE_$FH^\bullet$ | *20.90* | 5.49 | 2.18 | $2.08 \times 10^2$ |
| 14 | $HFP^\bullet$ + TFE → HFP_$TFE^\bullet$ | *2.91* | 4.42 | 2.10 | $1.17 \times 10^4$ |
| 15 | $TFE^\bullet$ + HFP → TFE_$HFP^\bullet$ | *14.94* | 5.45 | 2.42 | $1.66 \times 10^3$ |
| 16 | $TFE^\bullet$ + TFE → TFE_$TFE^\bullet$ | *10.55* | 6.02 | 2.57 | $3.06 \times 10^4$ |

[a]The rate coefficients were calculated at 60 °C. $FH^\bullet$: VDF tail radical. $HF^\bullet$: VDF head radical. HF, FH: VDF monomer. $HFP^\bullet$: HFP radical. HFP: HFP monomer. $TFE^\bullet$: TFE radical. TFE: TFE monomer. $k_{ij}$, i, j = FH, HF, HFP, TFE. The Arrhenius parameters were determined at the MPWB1K/6-31(d,p) level of theory.

reasonable. A second validation for the same set of kinetic parameters may be performed by comparing the obtained results with those proposed by Apostolo et al. using an appropriate mathematical model.[22] In this case, the computational estimations are 1 order of magnitude greater than the values estimated by the model. The activation energy of the monomeric radical addition is about 4−5 kJ/mol lower than the other three radicals addition reactions (Table S10, Supporting Information). Even if this difference is within the uncertainty limits of the method, it might be one of the reasons that the calculated $k_p$ is higher than the experimental results because the reaction rate increases exponentially when the activation energy decreases. Thus the chain length influence can be one of the possible causes for the overestimation of the $k_p$ values. Furthermore, one more validation of the adopted computational methodology may be performed on the basis of the experimental values for the kinetic coefficient of the TFE homopolymerization.[49] In particular, the $k_p$ values reported in the literature are 7400 and 9100 L/(mol·s) at 40 and 50 °C, respectively, whereas the calculated values at the MPWB1K level of theory are 20 500 and 25 300 L/(mol·s). Even in this case there is always an overestimation of the experimental data by less than 3 times. Considering all the sources of inaccuracies that may affect the computations, as well as the experimental conditions that cannot be reproduced using QM, the difference between the experiments and the computational data are within the range of current experimental uncertainty. Finally, reactivity ratios for VDF/HFP, VDF/TFE, and VDF/HFP/TFE systems have been estimated using the values in Table 3 considering only the VDF head radical. Despite the above-mentioned simplification, the obtained computational results are in acceptable agreement with the experimental values[19−21] whereas a better agreement is achieved when the VDF does not involve the calculations. For further information please refer to the Supporting Information.

## SCIENTIFIC CONCLUSIONS

A quantum mechanics investigation of the propagation reactions involved in all the possible binary copolymer systems including VDF, HFP, and TFE as terpolymerization monomers, as well as in the homopolymerization of VDF according to the terminal model, was conducted; the obtained results provided a comprehensive overview of these systems. The Arrhenius parameters and reactivity ratios were estimated by adopting two different levels of theory with good agreement between the data. The reliability of the computational methodology was demonstrated by comparing the computational predictions with the experimental values and model values found in the literature. The values in Table 3 indicate that the "head to tail" propagation (reaction 1) is more favorable than the "tail to head" (reaction 5) process that presents a kinetic constant 2 orders of magnitude smaller. The two cross propagation reactions (reaction 2 and 4), "head to head" and "tail to tail" were the same or higher importance than the "head to tail" propagation. In particular, the "head to head" propagation (reaction 2) provides a kinetic coefficient on the same order of magnitude, whereas, with its low activation energy and high pre-exponential factor, the "tail to tail" propagation of VDF (reaction 4) is the fastest reaction step. However, this result was expected because, during the "tail to tail" propagation, the less stable radical (radical on tail) produced a more stable radical (radical on head). For the VDF/HFP pseudo terpolymerization, the fastest propagation reactions (Scheme S1, Supporting Information) are the cross propagations (reactions 3 and 7): a VDF on head radical attacks a HFP monomer and a HFP radical adds to the methylene carbon on the VDF monomer. These reactions are characterized by low activation energies. However, according to the pre-exponential factors that may be calculated using the values reported in Table 3, the most probable propagation reaction is the "head to tail" (reaction 1) VDF homopolymerization that is characterized by a kinetic constant 2 orders of magnitude smaller than the constants of the previously mentioned cross propagation reactions. The pre-exponential factors for the propagation reactions in the VDF/TFE system (Scheme S2, Supporting Information) that may be calculated using the values in Table 3 do not differ significantly. Therefore, the propagation reactions with the lowest activation energies are the ones characterized by the higher kinetic coefficients. Finally, in accordance with the values reported in Table 3, TFE tends to homopolymerize, whereas HFP prefers to copolymerize in the HFP/TFE system. This is the only case where the behavior of the systems is different when estimated at two different levels of theory, even though the variations are not significant.

## ASSOCIATED CONTENT

### Supporting Information

Computational estimations for reactions kinetics of all the studied reactions at two different levels of theory (reactivity ratios, Arrhenius kinetic parameters, composition and rate coeeficients vs molar fraction), elementary reactions, chain length effect on activation energy, and details of the atom coordinates of the optimized transition state structures. This material is available free of charge via Internet.

## AUTHOR INFORMATION


### Corresponding Author

*D. Moscatelli: phone, +39-02-23993135; e-mail, davide.moscatelli@polimi.it.


### Notes

The authors declare no competing financial interest.

## ACKNOWLEDGMENTS


We thank Prof. Giuseppe Storti of ETH-Zurich for his continuous support and fruitful discussions. The research presented in this paper was supported by the European Union Seventh Framework Program (FP7/2007-2013) via Grant 238013.


## ABBREVIATIONS

VDF, vinylidene fluoride; HFP, hexafluoropropylene; TFE, tetrafluoroethylene; DFT, density functional theory; TM, terminal model; NMR, nuclear magnetic resonance; QM, quantum mechanics; PES, potential energy surface; TST, transition state theory

## REFERENCES


(1) Wall, L. A. *Fluoropolymers*; Wiley-Interscience: New York, 1971.

(2) Scheirs, J. *Modern Fluoropolymers: High Performance Polymers for Diverse Applications*; John Wiley & Sons: New York, 1997.

(3) Bloor, D. *The Encyclopedia of advanced materials*; Pergamon: Oxford, U.K., 1994.

(4) Ameduri, B.; Boutevin, B. *Well-Architectured Fluoropolymers: Synthesis, Properties and Applications*; Elsevier Science: Amseterdam, 2004.

(5) Ameduri, B. From Vinylidene Fluoride (VDF) to the Applications of VDF-Containing Polymers and Copolymers: Recent Developments and Future Trends. *Chem. Rev.* **2009**, *109*, 6632.
(6) Ebnesajjad, S. *Fluoroplastics: Vol. 2: Melt Processible Fluoropolymers - User's Guide and Databook*; Plastics Design Library: 2002.
(7) Moore, A. L. *Fluoroelastomers Handbook: The Definitive User's Guide*; Elsevier Science: Amsterdam, 2005.
(8) Souzy, R.; Ameduri, B.; Boutevin, B.; Gebel, G.; Capron, P. Functional fluoropolymers for fuel cell membranes. *Solid State Ionics* **2005**, *176*, 2839.
(9) Larsen, M. J.; Ma, Y.; Lund, P. B.; Skou, E. M. Crosslinking and alkyl substitution in nano-structured grafted fluoropolymer for use as proton-exchange membranes in fuel cells. *Appl. Phys. A: Mater. Sci. Process.* **2009**, *96*, 569.
(10) Hougham, G. G. *Fluoropolymers: Synthesis*; Kluwer Academic Publishers: Amsterdam, 1999.
(11) Banks, R. E.; Smart, B. E.; Tatlow, J. C. *Organofluorine Chemistry: Principles and Commercial Applications*; Springer: Berlin, 1994.
(12) Battiste, J. L.; Jing, N. Y.; Newmark, P. A. 2D F-19/F-19 NOESY for the assignment of NMR spectra of fluorochemicals. *J. Fluorine Chem.* **2004**, *125*, 1331.
(13) Duc, M.; Ameduri, B.; Boutevin, B.; Kharroubi, M.; Sage, J. M. Telomerization of vinylidene fluoride with methanol. Elucidation of the reaction process and mechanism by a structural analysis of the telomers. *Macromol. Chem. Phys.* **1998**, *199*, 1271.
(14) Isbester, P. K.; Brandt, J. L.; Kestner, T. A.; Munson, E. J. High-resolution variable-temperature F-19 MAS NMR spectroscopy of vinylidene fluoride based fluoropolymers. *Macromolecules* **1998**, *31*, 8192.
(15) Macheteau, J. P.; Oulyadi, H.; van Hemelryck, B.; Bourdonneau, M.; Davoust, D. 2D experiments for the characterization of fluorinated polymers: pulsed-field gradients H-1-F-19 hetero-COSY and its selective version. *J. Fluor. Chem.* **2000**, *104*, 149.
(16) Wormald, P.; Ameduri, B.; Harris, R. K.; Hazendonk, P. Fluorine-19 solid state NMR study of vinylidenefluoride polymers using selective relaxation filters. *Solid State Nucl. Magn. Reson.* **2006**, *30*, 114.
(17) Wormald, P.; Arneduri, B.; Harris, R. K.; Hazendonk, P. High-resolution F-19 and H-1 NMR of a vinylidenefluoride telomer. *Polymer* **2008**, *49*, 3629.
(18) Li, L. L.; Twum, E. B.; Li, X. H.; McCord, E. F.; Fox, P. A.; Lyons, D. F.; Rinaldi, P. L. 2D-NMR Characterization of Sequence Distributions in the Backbone of Poly(vinylidene fluoride-co-tetrafluoroethylene). *Macromolecules* **2012**, *45*, 9682.
(19) Gelin, M. P.; Ameduri, B. Radical solution copolymerisation of vinylidene fluoride with hexafluoropropene. *J. Fluorine Chem.* **2005**, *126*, 577.
(20) Moggi, G.; Bonardelli, P.; Bart, J. C. J. Copolymers of 1,1-difluoroethene with tetrafluoroethene, chlorotrifluoroethene, and bromotrifluoroethene. *J. Polym. Sci.: Polym. Phys. Ed.* **1984**, *22*, 357.
(21) Bonardelli, P.; Moggi, G.; Turturro, A. Glass transition temperatures of copolymer and terpolymer fluoroelastomers. *Polymer* **1986**, *27*, 905.
(22) Apostolo, M.; Arcella, V.; Storti, G.; Morbidelli, M. Kinetics of the emulsion polymerization of vinylidene fluoride and hexafluoropropylene. *Macromolecules* **1999**, *32*, 989.
(23) Siegmann, R.; Moller, E.; Beuermann, S. Propagation Rate Coefficients for Homogeneous Phase VDF-HFP Copolymerization in Supercritical CO2. *Macromol. Rapid Commun.* **2012**, *33*, 1208.
(24) Alfrey, T.; Goldfinger, G. Copolymerization of systems of three and more components. *J. Chem. Phys.* **1944**, *12*, 322.
(25) Dossi, M.; Liang, K.; Hutchinson, R. A.; Moscatelli, D. Investigation of Free-Radical Copolymerization Propagation Kinetics of Vinyl Acetate and Methyl Methacrylate. *J. Phys. Chem. B* **2010**, *114*, 4213.
(26) Dossi, M.; Storti, G.; Moscatelli, D. Initiation Kinetics in Free-Radical Polymerization: Prediction of Thermodynamic and Kinetic Parameters Based on ab initio Calculations. *Macromol. Theory Simul.* **2010**, *19*, 170.
(27) Van Speybroeck, V.; Van Cauter, K.; Coussens, B.; Waroquier, M. Ab initio study of free-radical polymerizations: Cost-effective methods to determine the reaction rates. *ChemPhysChem* **2005**, *6*, 180.
(28) Van Speybroeck, V.; Van Neck, D.; Waroquier, M.; Wauters, S.; Saeys, M.; Marin, G. B. Ab initio study of radical addition reactions: Addition of a primary ethylbenzene radical to ethene (I). *J. Phys. Chem. A* **2000**, *104*, 10939.
(29) Wong, M. W.; Radom, L. Radical addition to alkenes: Further assessment of theoretical procedures. *J. Phys. Chem. A* **1998**, *102*, 2237.
(30) Gomez-Balderas, R.; Coote, M. L.; Henry, D. J.; Radom, L. Reliable theoretical procedures for calculating the rate of methyl radical addition to carbon-carbon double and triple bonds. *J. Phys. Chem. A* **2004**, *108*, 2874.
(31) Peng, C. Y.; Ayala, P. Y.; Schlegel, H. B.; Frisch, M. J. Using redundant internal coordinates to optimize equilibrium geometries and transition states. *J. Comput. Chem.* **1996**, *17*, 49.
(32) Moscatelli, D.; Cavallotti, C.; Morbidelli, M. Prediction of molecular weight distributions based on ab initio calculations: Application to the high temperature styrene polymerization. *Macromolecules* **2006**, *39*, 9641.
(33) Moscatelli, D.; Dossi, M.; Cavallotti, C.; Storti, G. Density Functional Theory Study of Addition Reactions of Carbon-Centered Radicals to Alkenes. *J. Phys. Chem. A* **2011**, *115*, 52.
(34) Izgorodina, E. I.; Coote, M. L. Accurate ab initio prediction of propagation rate coefficients in free-radical polymerization: Acrylonitrile and vinyl chloride. *Chem. Phys.* **2006**, *324*, 96.
(35) Mavroudakis, E.; Liang, K.; Moscatelli, D.; Hutchinson, R. A. A Combined Computational and Experimental Study on the Free-Radical Copolymerization of Styrene and Hydroxyethyl Acrylate. *Macromol. Chem. Phys.* **2012**, *213*, 1706.
(36) Dossi, M.; Storti, G.; Moscatelli, D. Relevance of Backbiting and Beta-Scission Reactions in the Free Radical Polymerization of Acrylonitrile. *Macromol. Symp.* **2010**, *289*, 119.
(37) Hemelsoet, K.; Moran, D.; Van Speybroeck, V.; Waroquier, M.; Radom, L. An assessment of theoretical procedures for predicting the thermochemistry and kinetics of hydrogen abstraction by methyl radical from benzene. *J. Phys. Chem. A* **2006**, *110*, 8942.
(38) Yu, X. R.; Pfaendtner, J.; Broadbelt, L. J. Ab initio study of acrylate polymerization reactions: Methyl methacrylate and methyl acrylate propagation. *J. Phys. Chem. A* **2008**, *112*, 6772.
(39) Izgorodina, E. I.; Coote, M. L.; Radom, L. Trends in R-X bond dissociation energies (R = Me, Et, i-Pr, t-Bu; X = H, CH3, OCH3, OH, F): A surprising shortcoming of density functional theory. *J. Phys. Chem. A* **2005**, *109*, 7558.
(40) Becke, A. D. Density-Functional Thermochemistry. 3. The Role of Exact Exchange. *J. Chem. Phys.* **1993**, *98*, 5648.
(41) Lee, C. T.; Yang, W. T.; Parr, R. G. Development of the Colle-Salvetti Correlation-Energy Formula Into a Functional of the Electron Density. *Phys. Rev. B* **1988**, *37*, 785.
(42) Zhao, Y.; Truhlar, D. G. Hybrid meta density functional theory methods for thermochemistry, thermochemical kinetics, and noncovalent interactions: The MPW1B95 and MPWB1K models and comparative assessments for hydrogen bonding and van der Waals interactions. *J. Phys. Chem. A* **2004**, *108*, 6908.
(43) Heuts, J. P. A.; Gilbert, R. G.; Radom, L. Determination of arrhenius parameters for propagation in free-radical polymerizations: An assessment of ab initio procedures. *J. Phys. Chem.* **1996**, *100*, 18997.
(44) Sabbe, M. K.; Reyniers, M. F.; Van Speybroeck, V.; Waroquier, M.; Marin, G. B. Carbon-centered radical addition and beta-scission reactions: Modeling of activation energies and pre-exponential factors. *ChemPhysChem* **2008**, *9*, 124.
(45) Vansteenkiste, P.; Van Speybroeck, V.; Marin, G. B.; Waroquier, M. Ab initio calculation of entropy and heat capacity of gas-phase n-alkanes using internal rotations. *J. Phys. Chem. A* **2003**, *107*, 3139.
(46) Frisch, M. J.; Trucks, G. W.; Schlegel, H. B.; Scuseria, G. E.; Robb, M. A.; Cheeseman, J. R.; Scalmani, G.; Barone, V.; Mennucci,

B.; Petersson, G. A.; Nakatsuji, H.; Caricato, M.; Li, X.; Hratchian, H. P.; Izmaylov, A. F.; Bloino, J.; Zheng, G.; Sonnenberg, J. L.; Hada, M.; Ehara, M.; Toyota, K.; Fukuda, R.; Hasegawa, J.; Ishida, M.; Nakajima, T.; Honda, Y.; Kitao, O.; Nakai, H.; Vreven, T.; Montgomery, J. A.; Peralta, J. E.; Ogliaro, F.; Bearpark, M.; Heyd, J. J.; Brothers, E.; Kudin, K. N.; Staroverov, V. N.; Kobayashi, R.; Normand, J.; Raghavachari, K.; Rendell, A.; Burant, J. C.; Iyengar, S. S.; Tomasi, J.; Cossi, M.; Rega, N.; Millam, J. M.; Klene, M.; Knox, J. E.; Cross, J. B.; Bakken, V.; Adamo, C.; Jaramillo, J.; Gomperts, R.; Stratmann, R. E.; Yazyev, O.; Austin, A. J.; Cammi, R.; Pomelli, C.; Ochterski, J. W.; Martin, R. L.; Morokuma, K.; Zakrzewski, V. G.; Voth, G. A.; Salvador, P.; Dannenberg, J. J.; Dapprich, S.; Daniels, A. D.; Farkas, Ö.; Foresman, J. B.; Ortiz, J. V.; Cioslowski, J.; Fox, D. J. *Gaussian 09*, Revision B.01; Gaussian, Inc.: Wallingford, CT, 2009.

(47) Schaftenaar, G.; Noordik, J. H. Molden: a pre- and post-processing program for molecular and electronic structures. *J. Comput.-Aided Mol. Des.* **2000**, *14*, 123.

(48) Souzy, R.; Ameduri, B.; von Ahsen, S.; Willner, H.; Arguello, G. A. Use of bis(trifluoromethyl)peroxy dicarbonate as initiator in the radical homopolymerisation of vinylidene fluoride (VDF) and copolymerisation of VDF with hexafluoropropylene. *J. Fluorine Chem.* **2003**, *123*, 85.

(49) Plyusnin, A. N.; Chirkov, N. M. Use of stable radicals for the determination of rate constants of elementary processes. *Theor Exp Chem* **1966**, *2*, 563.